VARIATION IN MORPHOLOGY, HYGROSCOPICITY, AND OPTICAL PROPERTIES OF SOOT PARTICLES COATED BY DICARBOXYLIC ACIDS

A Thesis

by

HUAXIN XUE

Submitted to the Office of Graduate Studies of
Texas A&M University
in partial fulfillment of the requirements for the degree of

MASTER OF SCIENCE

May 2009

Major Subject: Atmospheric Sciences

VARIATION IN MORPHOLOGY, HYGROSCOPICITY, AND OPTICAL PROPERTIES OF SOOT PARTICLES COATED BY DICARBOXYLIC ACIDS

A Thesis

by

HUAXIN XUE

Submitted to the Office of Graduate Studies of
Texas A&M University
in partial fulfillment of the requirements for the degree of

MASTER OF SCIENCE

Approved by:

Chair of Committee,	Renyi Zhang
Committee Members,	Don Collins
	Simon North
Head of Department,	Kenneth Bowman

May 2009

Major Subject: Atmospheric Science

ABSTRACT

Variation in Morphology, Hygroscopicity, and Optical Properties of Soot Particles Coated by Dicarboxylic Acids. (May 2009)

Huaxin Xue, B.E., Donghua University, Shanghai, China;

M.S., Fudan University, Shanghai, China

Chair of Advisory Committee: Dr. Renyi Zhang

Soot aerosols are well known to be atmospheric constituents, but the hydrophobic nature of fresh soot likely prohibits them from encouraging cloud development. Soot aged through contact with oxygenated organic compounds may become hydrophilic enough to promote water uptake. In this study, the tandem differential mobility analyzer (TDMA) and differential mobility analyzer–aerosol particle mass analyzer (DMA–APM) were employed to measure the changes in morphology and hygroscopicity of soot aerosol particles upon coating with succinic and glutaric acids. The effective densities, fractal dimensions and dynamic shape factors of fresh and coated soot aerosol particles have been determined. Significant size-dependent increases of soot particle mobility diameter, mass, and effective density (ρ_{eff}) were observed upon coating of aggregates with succinic acid. These properties were restored back to their initial states once the acid was removed by heating, suggesting no restructuring of the soot core had occurred. Coating of soot with glutaric acid, on the other hand, leads to a strong size shrinking with a diameter growth factor ~0.60, even

after the acid has been removed by heating suggesting the strong restructuring of the soot agglomerate. The additional 90% RH cycle can evidently enhance the restructuring process.

The extinction and scattering properties at 532 nm of soot particles internally mixed with dicarboxylic acids were investigated experimentally using a cavity ring-down spectrometer and an integrating nephelometer, respectively, and the absorption is derived as the difference between extinction and scattering. It was found that the organic coatings significantly affect the optical and microphysical properties of the soot aggregates. The size-dependent amplification factors of light scattering were as much as 3.8 and 1.7 with glutaric and succinic acids coatings, respectively. Additional measurements with soot particles that are first coated with glutaric acid and then heated to remove the coating show that both scattering and absorption are enhanced by irreversible restructuring of soot aggregates to more compact globules. These results reveal the microphysical state of soot aerosol with incomplete restructuring in the atmosphere, and advance the treatment of atmospheric aged soot aerosol in the Mie theory shell-and-core model.

ACKNOWLEDGEMENTS

I would like to thank my committee chair, Dr. Renyi Zhang, for teaching me how to use my knowledge of chemistry to expand the horizons of human understanding.

I would also like to thank my committee members, Dr. Don Collins and Dr. Simon North, for their wonderful teaching ability, and general advising assistance.

This work was supported by the US Department of Energy National Institute for Climate Change Research (DOE-NICCR) and the Robert A. Welch Foundation.

I would like to show special appreciation toward Dr. Alexei Khalizov for sharing his world of knowledge with me, sometimes more than I asked for. I am also grateful for the assistance, comments, and suggestions from the rest of Dr. Zhang's research group. Our time together has been a great experience for me.

Finally, I want to recognize my friends and family for their unfailing support and patience.

TABLE OF CONTENTS

Page

ABSTRACT ……iii

ACKNOWLEDGEMENTS ……..v

TABLE OF CONTENTS …….....vi

LIST OF TABLES ……..vii

LIST OF FIGURES ……viii

1. INTRODUCTION…….....1

2. EXPERIMENTAL……..7

2.1. Generation and Sampling of Soot Aerosol …….....7
2.2. Coating and Conditioning of Soot Aerosol ……...9
2.3. Tandem DMA (TDMA) ……..11
2.4. DMA–APM …….....11
2.5. Measurements of Aerosol Optical Properties ……12
2.6. Multiply-charged Particles in Soot Aerosol ……15

3. MORPHOLOGY AND HYGROSCOPIC GROWTH OF SOOT PARTICLES….....17

3.1. Mass-Mobility Relationship …….....17
3.2. Inherent Material Density and Dynamic Shape Factor …….....27
3.3. Atmospheric Implications …….....30

4. ENHANCED OPTICAL PROPERTIES OF SOOT PARTICLES ……31

4.1. Optical Properties of Fresh and Coated Soot Aggregates ……...31
4.2. Enhancement Mechanism …….....35
4.3. Atmospheric Implications …….....40

5. CONCLUSIONS……..43

REFERENCES ……45

VITA…….53

LIST OF TABLES

Page

Table 1 Dicarboxylic acids investigated.…….....10

Table 2 Mass-specific absorption cross-sections of soot aerosol (λ = 532 nm) before and after exposure to glutaric acid and succinic acid vapor……..40

LIST OF FIGURES

Page

Figure 1 Schematic of the TDMA and DMA-APM system……7

Figure 2 Typical size distribution for the soot aerosol used in this study. The measured distribution was well reproduced with a constant fuel/air ratio……8

Figure 3 Schematic diagram of the experimental setup for measurements of light extinction and scattering by soot particles……...13

Figure 4 Mobility diameter (a) and mass (b) growth factors of soot and PSL particles upon coating by succinic acid. Measurements were performed with initial diameters of 50, 80, 150, 240, and 350 nm…….18

Figure 5 Effective densities of fresh and succinic acid-coated soot particles as a function of processed mobility diameter. The fractal dimension (D_f) was obtained using equation (1)…….…...19

Figure 6 Mobility diameter (a) and mass (b) growth factors of soot and PSL particles upon coating by glutaric acid. Measurements were performed with initial diameters of 50, 80, 150, 240, and 350 nm…….21

Figure 7 Effective densities of fresh and glutaric acid-coated soot particles as a function of processed mobility diameter. The fractal dimension (D_f) was obtained using equation (1)……...24

Figure 8 A schematic diagram showing the difference of morphology behaviors of soot aggregates with coatings of succinic and glutaric acids…….....25

Figure 9 The dynamic shape factors as a function of mobility diameter for fresh and coated soot (SA = succinic acid, GA = glutaric acid)……..29

Figure 10 Temporal profile of the extinction, scattering, and absorption cross-sections of soot aerosol (λ = 532 nm) after exposure to the glutaric acid vapor (8.5×10^{12} molecule cm^{-3}). The initial particle mobility diameter is 245 nm and relative humidity is 5%.....31

Figure 11 Amplification factors of soot scattering, and absorption

Page

cross-sections (λ = 532 nm) after exposure of aerosol to the glutaric acid vapor (8.5×10^{12} molecule cm^{-3}) at 5% RH or an additional 90% RH cycle. The initial (uncoated) particle mobility diameters are 155, 245, and 320 nm…….....32

Figure 12 Amplification factors of soot scattering, and absorption cross-sections (λ = 532 nm) after exposure of aerosol to the succinic acid vapor (4.4×10^{13} molecule cm^{-3}) at 5% RH or an additional 90% RH cycle. The initial (uncoated) particle mobility diameters are 155, 245, and 320 nm…….....34

Figure 13 Variations in light scattering and absorption (λ = 532 nm) by soot agglomerates subjected to different types of processing (a) exposed to the glutaric acid and (b) exposed to the succinic acid. "Fresh" stands for uncoated soot aerosol, "heated" for soot aerosol that is heated to 200 °C, "coated" for soot aerosol that is exposed to acid vapor, "coated&heated" for soot aerosol that is exposed to acid vapor and subsequently heated to 200°C. The initial (uncoated) soot particle mobility diameters are 155, 245, and 320 nm and relative humidity is 5% RH…….36

1. INTRODUCTION

Soot particles are ubiquitous in the troposphere and are of current interest because of their ability to force global climate by altering cloud formation (Ackerman et al., 2000) and Earth radiation balance (Jacobson, 2001). Soot is produced directly by incomplete combustion of fossil fuel and biomass at a global emission rate of 8–24 Tg C yr^{-1} (Penner et al., 1993; Bond et al., 2004). The freshly emitted soot particles are typically hydrophobic and hence unlikely to act as cloud condensation nuclei (CCN). However, chemical and physical aging processes occurring during transport can alter the role of soot in the atmosphere. An understanding of soot aging and its effects on particle hygroscopicity, morphology, and composition is necessary to address the direct and indirect effects of soot on climate.

Soot particles are emitted as complex aggregates and their structure is directly related to their atmosphere fate and deposition efficiency in the human respiratory system. The fractal dimension (D_f) is an indirect measure of the morphology of irregularly shaped agglomerated particles. It varies in the range of 1 to 3, with $D_f = 3$ for compact spheres, and $D_f = 1$ in the limit of infinitely long straight chain agglomerates (DeCarlo et al., 2004). D_f can be defined and calculated in several different ways. McMurry et al. (2002) and Park et al. (2003) developed a technique, which uses simultaneous Differential Mobility Analyzer (DMA) and Aerosol Particle Mass analyzer

---

This thesis follows the style and format of the *Journal of Aerosol Science*.

(APM) measurements to determine the effective density and fractal dimension of gas-borne particles from the relationship between their electrical mobility diameter and mass. The mass-fractal dimension, D_f, based on mobility diameter, d_{me}, and particle mass, m, is defined as:

$$m \propto d_{me}^{D_f} \quad (1)$$

It has been shown that aging of soot particles may occur by the uptake of soluble inorganic and organic compounds such as H_2SO_4 (Pagels et al., 2008; Zhang and Zhang, 2005; Zhang et al., 2008), HNO_3 (Zuberi et al., 2005), and organic acids (Levitt et al., 2007; Mikhailov et al., 2006), making soot hydrophilic. Mikhailov et al. (2006) found that the hydrophobic soot particles do not exhibit any structural or morphological differences under dry and saturated conditions, whereas hydrophilic particles prepared by coating soot with glutaric acid collapse into globules when relative humidity is increased to saturation, and the extent of this change depends on the mass fraction of coated material. Weingartner et al. (1997) have shown that carbon soot aggregates from spark discharge collapse to compact structures at high RH, but the diesel combustion particles exhibit a much smaller restructuring. Only limited restructuring was observed by Environment Scanning Electron Microscope (ESEM) when diesel soot particles were exposed to three supersaturated relative humidity cycles (Huang et al., 1994). Diesel soot particles are often observed to have hydrophobic organic coating composed primarily of lubricating oil, unburned hydrocarbons, and PAHs (Park et al., 2003). Field measurements have shown that typical low-molecular weight dicarboxylic organic acids, such as succinic and glutaric acids, are a significant component of fine particulate matter

in the troposphere (Saxena and Hildemann, 1996). Coating soot with dicarboxylic acids can transform the particles from hydrophobic to hydrophilic. However, few studies have considered soot aging upon interaction with organic acids and the corresponding changes of hygroscopicity and morphology (Mikhailov et al., 2006).

In this work, I have studied the propane flame-generated soot aerosol particles coated by succinic and glutaric acids. The effect of coating on the mobility diameter and mass of size-classified aerosol was measured by tandem-DMA (TDMA) and DMA–APM techniques, respectively. The mobility-mass relationship allowed us to determine the effective density, fractal dimension, and dynamic shape factor of soot before and after processing, which included coating with dicarboxylic organic acids, exposure to water vapor, and heating.

Atmospheric aerosols are also known to directly affect the solar radiation balance in the atmosphere by scattering and absorbing incoming light. Many previous studies have focused on the complex mixtures including mineral dust, inorganic and organic compounds, and soot aerosol (Tegen et al., 1996; Kaufman et al., 2002; Jacobson, 2001; Ramanathan and Carmichael, 2008). Of these, soot particularly attracts considerable attentions because of its effective light absorbability, and the internally and externally mixed aerosol containing soot contributes to climate change by direct radiative forcing (IPCC, 2007). Absorbing aerosol can heat the atmosphere and lead to global warming. It is necessary to measure optical properties of soot-containing aerosols and evaluate the effect on climate change. Moreover, Soot is the dominant absorber of visible solar radiation in the atmosphere. Hence, the optical properties of soot-containing aerosols

directly impact the atmospheric visibility as well as regional air quality (Shiraiwa et al., 2007).

The optical properties of aerosols are dominated by their chemical composition and physical characteristics, such as shape and morphology, which lead to large uncertainties in quantifying changes in the climate system. Moreover, freshly hydrophobic soot is subjected to various aging processes in the atmosphere including externally and internally mixed with various atmospheric species. The aging process can also affect the morphology of soot by collapsing into a more compact or near-sphere morphology (Khalizov et al., 2008b). These processes may happen readily in polluted areas. Hydrophilic coatings can significantly change soot's fate in the atmosphere and potential of acting as cloud condensation nuclei (CCN) (Nenes et al., 2002). The specific absorption cross-section and hence the radiative heating potential of atmospheric soot aerosol may significantly be enhanced by internal mixing with organic or inorganic compounds (Mikhailov et al., 2006; Zhang et al., 2008). The light absorbability of soot can be enhanced by a factor of about 1.5 if soot is thickly coated with non-refractory compounds (Bond et al., 2006).

The effects of soot on climate are often modeled by a spherical shape based on Mie theory. However, large uncertainty may be associated with enhanced absorption because of the difficulty in modeling the optical properties of morphologically complex aerosols and the paucity of direct measurements constraining soot mixing state in the atmosphere (Schwarz et al., 2008). Fuller et al. (1999) found that aggregation of fine spherules alone can increase soot absorption by 30%, and encapsulation of soot particle

within a sulfate host may further increase soot absorption by the factor of 2. Furthermore, soot randomly positioned within sulfate droplets can display averaged absorption enhancement factors of about 2.5–4.0. Jacobson (2001) simulated the evolution of the chemical composition of internally mixed soot and found that the warming effect of internally mixed soot is stronger than in the externally mixed state and even more than soot alone. Since soot aggregate usually undergoes a significantly restructuring during atmospheric aging resulting in more compact core, it is difficult or even feasible to calculate the optical properties of such complex-structured particles.

To better understand the effect of absorbing soot aerosol on climate, it is required to quantitatively characterize the optical properties of internally mixed soot aerosols. Despite of the challenging quantitative measurements of soot optical properties, there are a few laboratory measurements of internally mixed state soot optical properties have been investigated. Khalizov et al. (2008a) recently reported the significant amplification of light absorption and scattering by carbon soot particles internally mixed with sulfuric acid, as well as the morphology, mixing state, and hygroscopic properties of these particles. For soot particles with an initial mobility diameter of 320 nm and a 40% H_2SO_4 mass coating fraction, absorption and scattering are increased by 1.4– and 13–fold at 80% RH, respectively. Schnaiter et al. (2005) reported the absorption amplification factors of 1.8 to 2.1 for the internally mixed soot with ozonolysis products of α-pinene. These factors can be well reproduced by a Mie model over a wide range of organic coating/black carbon mixing ratio. Mikhailov et al. (2006) produced hydrophilic soot by internally mixed with glutaric acid in laboratory. The maximum enhancement in

absorption for this kind of soot was as much as a factor of 3.5, very similar to theoretical predictions. Further laboratory studies with more representative atmospheric organic species (such as soluble dicarboxylic acids) need to be performed to parameterize soot microphysical processes and improve the climate models predictive capabilities.

In this study I present the use of cavity ring-down spectrometer (CRDS) and Nephelometer for in-situ measurements the extinction and scattering cross-sections, respectively. The soot aerosol was produced from a propane diffusion flame and internally mixed soot with glutaric and succinic acids, which are non-absorbing organic compounds found abundantly in atmospheric aerosols. By combining measurements of particle mobility size and mass (Xue et al., 2008a), I draw fundamental conclusions of atmospheric processing on the optical properties and effects on regional air quality and radiative balance.

2. EXPERIMENTAL

The details of the experimental set-up used to measure the optical properties of soot-containing aerosols have been reported previously (Xue et al., 2008a, 2008b). The experimental facilities employed in this study provide aerosol generation, sizing, processing and optical measurements of soot particles under various humid conditions. The soot particles were size-selected using a differential mobility analyzer (Long DMA 3081, TSI Inc.), and passed through the aerosol particle mass analyzer (APM) for mass-mobility relationship measurements, or Nephelometer (3563, TSI Inc.) and cavity ring-down spectrometer (CRDS) cell for optical measurements. The particles were counted at the exit of the APM or CRDS cell with a condensation particle counter (CPC, 3076A, TSI Inc.).

2.1. Generation and Sampling of Soot Aerosol

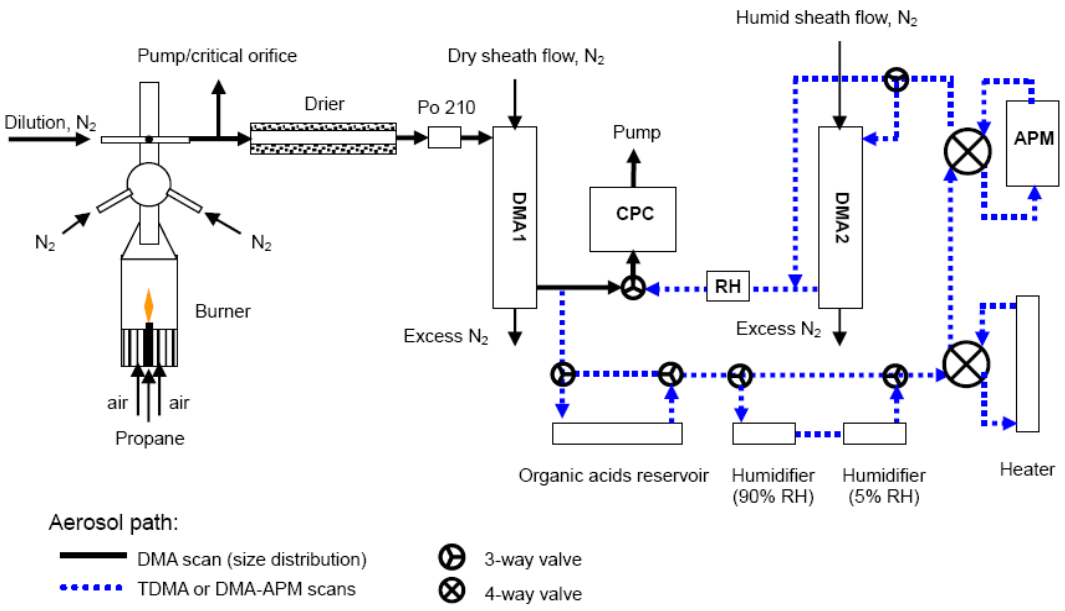

Figure 1. Schematic of the TDMA and DMA-APM system.

A schematic of our experimental setup is shown in Figure 1. Soot aerosol was generated with a Santoro-type laminar diffusion burner by combustion of propane (Santoro et al., 1983). The soot sampling system consists of a horizontally mounted stainless steel tube with a 1 mm orifice. Coagulation of the primary particles led to formation of submicron size soot fractal aggregates with geometric mean diameter of 130 nm and geometric standard deviation of 1.8. Two crossing dilution N_2 flows at the top of the burner provided uniform mixing and dilution of soot and prevented further coagulation. Soot aerosol was diluted by a 7 LPM N_2 carrier gas flow and then passed through a diffusion drier and a Nafion drier to reduce the RH to below 1%. A flame equivalence ratio was used throughout this study to maintain a constant size distribution with a geometric mean diameter of 130 nm. The typical size distribution is shown in

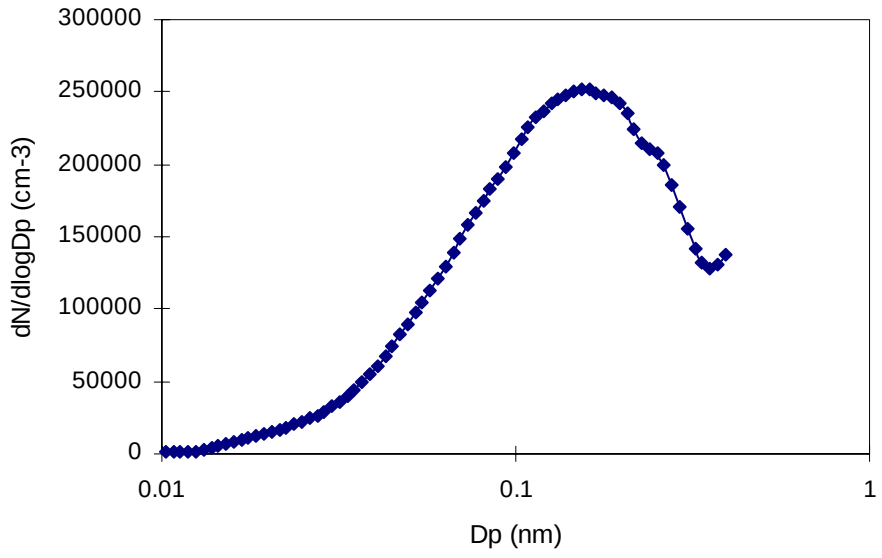

Figure 2. Typical size distribution for the soot aerosol used in this study. The measured distribution was well reproduced with a constant fuel/air ratio.

Figure 2. Polystyrene latex (PSL, Duke Scientific Inc., USA) aerosol was produced by nebulizing suspension of spheres in deionized water (17 MΩ) using an atomizer (Model 376001, TSI Inc.).

2.2. Coating and Conditioning of Soot Aerosol

The fresh soot aerosol passed through a Po-210 bipolar charger and entered the first DMA, where the particles with a known size were selected. Mobility-classified aerosol passed over a heated reservoir with desired coating material. Table 1 summary atomic formulas, molecular weights, water solubility, and vapor pressure of the low weight dicarboxylic acids. Glutaric and succinic acids were used in this study because of their moderate solubility and vapor pressures, as well as the significant amounts observed in the atmosphere. Glutaric acid (Sigma, 99%), and succinic acid (Sigma, 99%) were used as received without further purification.

The organic vapor was entrained into the aerosol flow where it condensed on the particle surface upon cooling to room temperature. The upper limit of dicarboxylic acid concentration in the coating reservoir was estimated from thermodynamic data (Bilde et al., 2003; Mönster et al., 2004) to be 4.4×10^{13} molecule cm^{-3} for succinic acid, and 8.5×10^{12} molecule cm^{-3} for glutaric acid. The residence time in the reservoir was 20 s. To study the effect of relative humidity, coated soot aerosol was passed through a 90% RH humidifier and then dried to ~5% RH. Also coated and humidified/dried soot aerosol could be heated to 200 °C to remove the organic coating.

Table 1. Dicarboxylic acids investigated

Compounds	Chemical formula	Molecular weight	Density (g/cm3)	Solubility (mg/L, 25 °C)	Vapor pressure (Torr)	Surface tension (dyn/cm) [c]
Oxalic acid	HOOC-COOH	90.04	1.9	2.2×10^{5}	3.5×10^{-5}	--
Malonic acid	HOOC-(CH2)-COOH	104.06	1.63	7.6×10^{5}	1.0×10^{-5}	-1.56
Succinic acid	HOOC-(CH2)2-COOH	118.09	1.57	8.3×10^{4}	6.9×10^{-7} [a] 7.9×10^{-6} [b]	-2.91
Glutaric acid	HOOC-(CH2)3-COOH	132.12	1.43	1.6×10^{6}	4.1×10^{-6} [a] 7.78×10^{-6} [b]	-6.61
Adipic acid	HOOC-(CH2)4-COOH	146.14	1.36	3.2×10^{2}	1.5×10^{-7}	-7.26

[a] The values at 30 °C from Prenni et al. (2001).

[b] The values at 25 °C from Saxena and Hildemann (1996).

[c] Surface tension of aqueous solution $\Delta\gamma$, dyn/cm, (at 0.15~0.25 mol per kg water).

2.3. Tandem DMA (TDMA)

TDMA (Long DMA 3081, TSI Inc.) was employed to measure the mobility size change of soot aerosol particles upon coating with organic acids. We used DMA1 to mobility-classify the fresh soot aerosol before further passing it through organic acid reservoir. The TDMA was operated at a sheath flow rate of 6.5 LPM N_2 and sample flow 1.0 LPM. The system allowed relative humidity control in the range 2–95% and automated data acquisition. Measurements with bypassed coating reservoir were used to correct for the small offset between DMA1 and DMA2 for both soot and PSL. The diametric growth factor, Gfd, was defined as the ratio of coated soot mobility diameter measured by DMA2 to the fresh soot diameter selected by DMA1.

2.4. DMA–APM

The APM (APM-3600, Kanomax Inc., Japan) technique has been described in detail previously (McMurry et al., 2002; Ehara et al., 1996). In contrast to electrical mobility-based classification of particles by DMA, in APM particles are selected according to their mass, independently of shape. The mass of a particle that passes through the APM is determined by the rotational speed and applied voltage. Different rotational speeds (1500–9000 rpm) are used to measure the particles in the size range from 50 nm to 350 nm. For each rotation speed, the voltage is stepped and the concentration of particles passing through APM is measured by CPC (Model 3760, TSI Inc.). As described by McMurry et al. (2002), experiments are first carried out for spherical PSL particles with known size and material density to calibrate the

DMA–APM system. The DMA1 flow rates and classifying voltage are held fixed for measurements involving PSL and soot particles to ensure that the selected mobility sizes are identical. Similarly, the APM rotational speed is held fixed while measuring PSL and soot particles. This methodology reduces measurement uncertainties that might lead to a large error in density calculation. The effective density is determined by

$$\rho_{eff} = \frac{V_{APM,soot}}{V_{APM,PSL}} \cdot \rho_{PSL}, \quad (2)$$

where $V_{APM, soot}$ and $V_{APM, PSL}$ are the APM classifying voltage distribution peaks for soot and PSL particles, ρ_{PSL}=1.054 g cm^{-3} is the inherent material density of Polystyrene latex. The effects of conditioning on particle mobility and mass are then studied. The mass of fresh (m_{fresh}) and coated (m_{coated}) soot are always measured in the adjacent cycles to minimize effects of small variations. Mass growth factor is then defined as

$$Gfm = \frac{m_{coated}}{m_{fresh}}. \quad (3)$$

The mass fractal dimension of fresh and coated soot is calculated from the measured mobility diameter and mass using equation (1).

2.5. Measurements of Aerosol Optical Properties

Soot aerosol scattering property was measured directly by a commercial three-wavelength (450, 550, and 700 nm) integrating Nephelometer (3563, TSI Inc.). The scattering coefficient at 532 nm was calculated from a power law fit to the scattering coefficients at the three Nephelometer wavelengths.

The extinction efficiency of soot aerosol particles was measured by a CRDS apparatus, which consisted of two highly reflective concave mirrors (540 nm center wavelength, 99.9985% reflectivity, 6 m radius of curvature, 0.8" diameter, Los Gatos Research, Inc.). A small dry nitrogen purge flow (20 mL/min) was introduced to each mirror to prevent contamination from particle deposition. The system was described elsewhere (Khalizov et al., 2008a) and only a diagram about CRDS setup is shown in

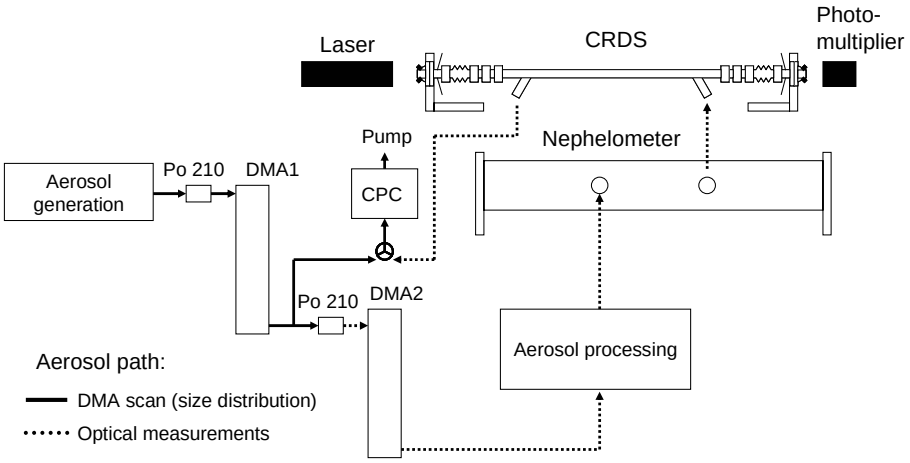

Figure 3. Schematic diagram of the experimental setup for measurements of light extinction and scattering by soot particles.

Figure 3. A light pulse at 532 nm (pulse energy 100 μJ, pulse duration 11 ns) produced by a Q-switched pulsed laser (CrystaLaser QG-532-500) was injected into a CRDS cell. The ring down signal through the output mirror was measured with a photomultiplier (Hamamatsu H6780-02). The output of the photomultiplier was digitized by a 16 bit resolution CompuScope 12100 card (100 MHz, GaGe Applied Technologies, LLC) operated by LabVIEW program.

When the CRDS cell was filled with absorbing or scattering particles, the light intensity was decayed due to the light extinction, which resulted in a ring down trace with a shorter time scale. The light extinction coefficient, b_{ext}, can be calculated using the difference of decay times with and without the aerosol sample according to the equation

$$b_{ext} = \frac{R_L}{c}\left(\frac{1}{\tau} - \frac{1}{\tau_0}\right) \tag{4}$$

where R_L is the ratio of optical cavity length to sample length, c is the speed of light, τ is the ring-down time with sample present, and τ_0 is the ring-down time in the absence of sample.

The absorption coefficient is calculated from the difference between the extinction and scattering coefficients. The particle number density measured by CPC is used together with extinction, scattering, and absorption coefficients to calculate the corresponding cross-sections

$$C = \frac{b}{N} \tag{5}$$

where C is the cross-section and N is the particle number density. The particle losss in CRDS cell are negligible. To calibrate particle losses in the nephelometer, size-dependent transmission coefficients were applied to particle concentrations measured by CPC. By selecting a monodisperse aerosol size and measuring the particle number density N, the extinction, scattering, and absorption cross section can be determined by this way. Mass-specific absorption cross-sections, σ_{abs}, is a very important

factor to evaluate the light absorbability of soot, which can be calculated using the following equation

$$\sigma_{abs} = \frac{C_{abs}}{m_p} \tag{6}$$

where m_p is the mass of soot particle, which has been measured by DMA-APM (Aerosol Particle Mass) analyzer under the identical conditions to those used in our previous experiments.

2.6. Multiply-charged Particles in Soot Aerosol

The dried soot (PSL) particles were charged with two 20 mCu Po 210 sources and passed through a single DMA to select a nearly monodisperse size distribution. The particles were sized according to their electrical mobility in DMA. However, in practice, the formation of multiply charged particles yielded a sequence of discrete particle sizes at the DMA exit. The mobility diameters of multiply charged particles have a ratio of $n^{1/2}$ to that of the singly charged particles. Multiply-charged particles, because of their larger effective size, scatter and absorb light more efficiently than singly-charged particles of the same electrical mobility. Since optical properties vary non-linearly with the particle size, even a small fraction of these larger particles in aerosols can lead to significant overestimation of the measured optical cross-sections.

In the case of PSL particles, the DMA voltage was set accordingly to transmit singly charged particles. All impurities, multiply charged PSL particles, and coagulated spheres were removed within the DMA. The presence of multiply-charged soot particles

in the mobility-classified aerosol can be revealed by using an additional charger and a second DMA in series with DMA1. More details about multiply-charged particles and comparisons with Mie theory calculation have been shown in our previous study (Khalizov et al., 2008a). In this study, I used the same mobility size of 155, 245, and 320 nm.

3. MORPHOLOGY AND HYGROSCOPIC GROWTH OF SOOT PARTICLES

3.1. Mass-Mobility Relationship

Succinic acid. The mobility diameter growth factors for PSL and soot particles coated by succinic acid are given in Figure 4(a). Succinic acid has low vapor pressure at room temperature and thus its evaporation from coated particles is negligible. Under dry conditions, the mobility diameters of soot and PSL particles increase upon coating by succinic acid and smaller particles exhibit larger growth. When coated soot particles are subjected to a high RH cycle through humidification to 90% RH and subsequent drying to 5% RH, their mobility diameter decreases by 2–6%, stronger shrinking for larger particles. Coated soot aggregates subjected to high RH cycle and subsequent heating to remove succinic acid show growth factors ranging from 0.95 to 0.97. Without humidification, however, heating the coated soot aerosol leads to growth factors 0.97–0.99. The observed behavior can be caused by restructuring of the soot cores and/or filling up the core voids by succinic acid aqueous solution formed at high RH. Even though succinic acid is expected to be solid below its deliquescence point, 99% RH (Peng et al., 2001; Prenni et al., 2001), several monolayers of water condensed on the hydrophilic acid surface can lead to small compaction of the coated aggregates.

For spherical particles, such as PSL, the diametric growth factor provides an indication of the coating volume fraction. In the case of soot aggregates, however, the condensing material can fill up the voids between the primary spheres and the change in the mobility diameter may have a complex relation with the coating fraction. Thus, even in the absence of compaction of the soot cores, methods capable of direct

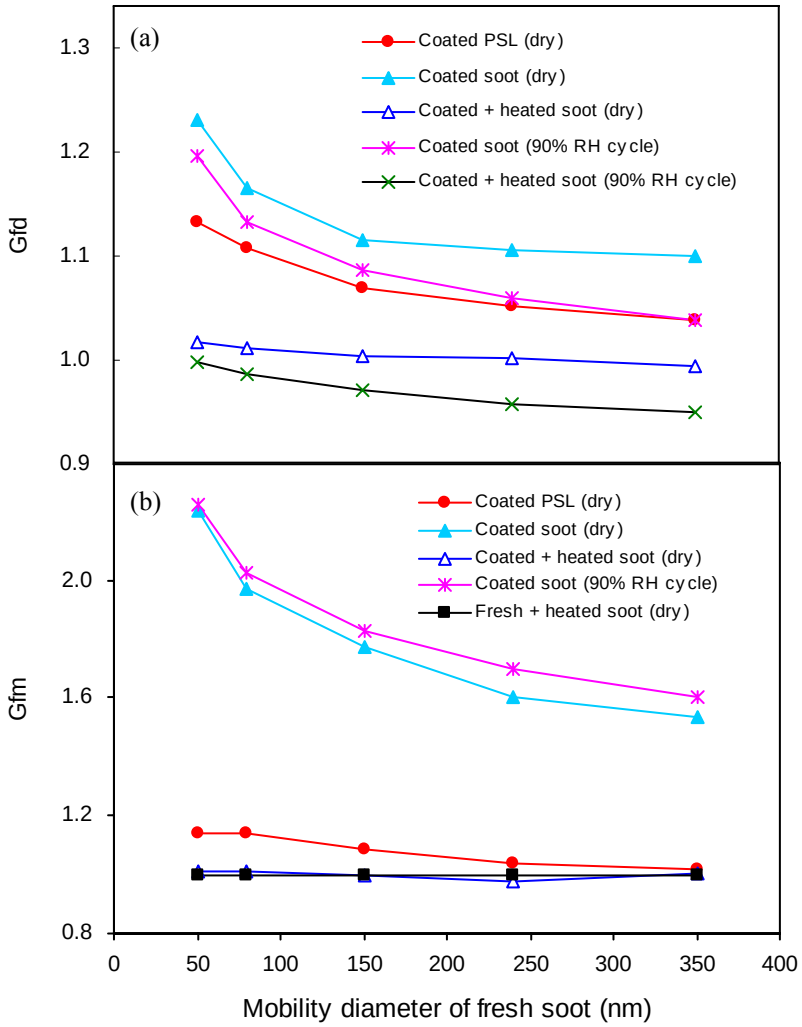

Figure 4. Mobility diameter (a) and mass (b) growth factors of soot and PSL particles upon coating by succinic acid. Measurements were performed with initial diameters of 50, 80, 150, 240, and 350 nm.

measurement of the coating volume or mass need to be employed to characterize the mixing state of coated particles. The APM measurements show that the coated soot particles contain 35–55% succinic acid by mass with the corresponding mass growth factors ranging from 1.53 to 2.24 (Figure 4(b)). The decreasing mass growth for particles

with larger initial size is in agreement with the trend observed for sulfuric acid-coated soot particles (Pagels et al., 2008). The mass growth factor of heated fresh soot is 0.99±0.05, indicating that the fraction of material volatile at 200 ºC, e.g. organic carbon, is negligible for the propane soot produced in our study. When the coated soot is passed through the heater, the mass ratio of coated to fresh soot is reduced to 1.00±0.05, illustrating that condensed glutaric acid can be removed efficiently and no chemical interaction takes place. The high RH cycle measurements show a small but reproducible mass increase of coated soot particles, indicating that a small amount of water vapor absorbed at 90% RH remains in the coating even after drying the particles to 5% RH.

The data on the mass-mobility relationship allow us to calculate the effective densities of fresh and coated soot aggregates. The effective density of fresh soot

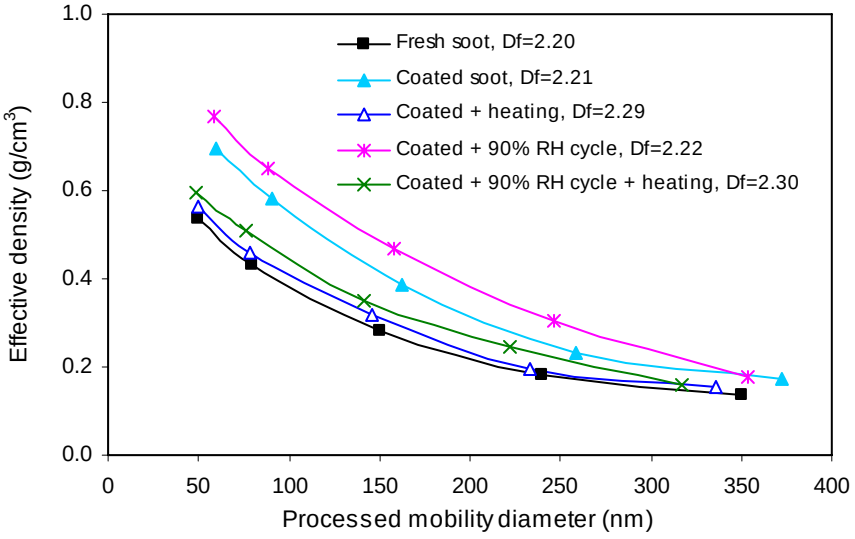

Figure 5. Effective densities of fresh and succinic acid-coated soot particles as a function of processed mobility diameter. The fractal dimension (D_f) was obtained using equation (1).

decreases with the increasing mobility size (Figure 5). Once coated with organic acid, the aggregates effective density increases, but remains significantly lower that the inherent bulk density of either soot or succinic acid. The values of fractal dimension determined using equation (1) show a small variation between fresh (D_f = 2.20) and coated (D_f = 2.21) soot. On the contrary, coated and heated soot has increased fractal dimension under both dry (D_f = 2.29) and high RH cycle (D_f = 2.30) conditions. The small restructuring of coated aggregates upon heating to 200 °C can be caused by the melted succinic acid (melting point is 185 °C).

Park et al. (2003) have shown a decrease in fractal dimension of diesel soot from 2.41 to 2.33 with increasing engine load from 10% to 75% because of higher condensation of oil at lower loads. Maricq and Xu (2004) described the typical D_f values of 2.15 for flame-generated soot and 2.30 for diesel exhaust particulate matter. D_f values for propane soot measured by DMA and Aerodyne aerosol mass spectrometer (AMS) were found to depend on the fuel equivalence ratio, increasing from 1.7 (lower propane/O_2) to 2.95 (high propane/O_2) due to condensation of the incomplete combustion products on the soot particles (Slowik et al., 2004). Geller et al. (2006) used DMA–APM setup to find that D_f was about 2.4–2.5 for freshly emitted soot nearby two freeways. In Riverside and Coast areas which are away from traffic emissions, fractal dimensions were found to increase to 2.8–3.0, indicating aging of soot particles during atmospheric transport. Pagels et al. (2008) observed the mass fractal dimension of fresh soot generated from propane flame to increase from 2.11 to 2.80 after coating by sulfuric acid with a mass fraction of 55%. Unlike other condensing materials, succinic acid does

not significantly increase the fractal dimension of soot aggregates because little restructuring takes place upon coating.

Glutaric acid. Another set of experiments was conducted using glutaric acid as condensable material. The changes in mobility diameter of PSL and soot particles

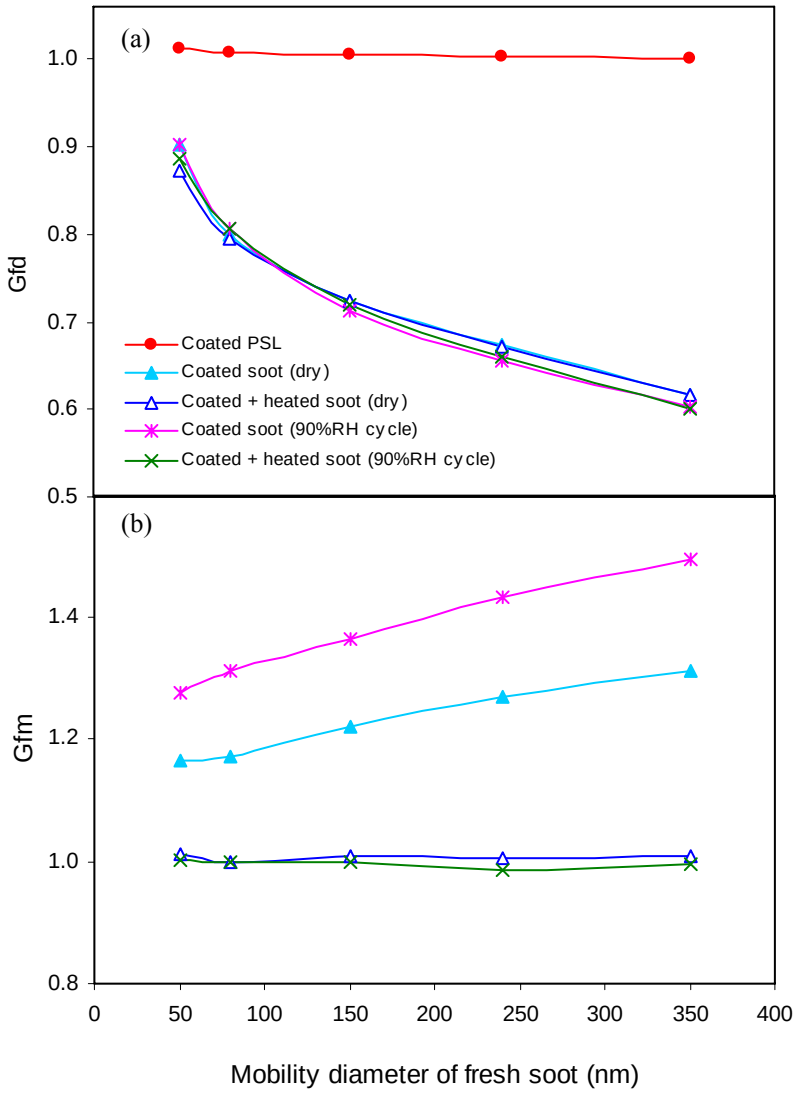

Figure 6. Mobility diameter (a) and mass (b) growth factors of soot and PSL particles upon coating by glutaric acid. Measurements were performed with initial diameters of 50, 80, 150, 240, and 350 nm.

exposed to glutaric acid are given in Figure 6(a). The mobility diameter of soot aggregates decreases by 10–40% upon coating, suggesting that internal mixing with glutaric acid significantly alters the soot morphology. The shrinking effect is more significant for agglomerates with larger initial mobility size and lower density. After acid is removed by heating, particle size does not recover to initial value and hence the restructuring is irreversible. The spherical PSL particles always show slightly increased mobility diameter upon condensation of glutaric acid. The high humidity cycle does not promote any further change in the size of coated soot particles, indicating that the complete restructuring can be achieved in the presence of glutaric acid coating without participation of water.

Figure 6(b) illustrates changes in the particle mass upon coating of soot with glutaric acid as a function of initial mobility diameter. The mass growth factors vary between 1.17 and 1.31 under dry condition, which corresponds to 14–24% glutaric acid fraction of the coated particle mass. Heating the coated particles completely removes glutaric acid (mass growth factor 1.00±0.05), in full agreement with the results of a fast flow reactor study (Levitt et al., 2007), which reported a reversible uptake of glutaric acid on soot.

Mass growth factor of glutaric acid-coated soot increases with the initial particle size (Figure 6(b)), which is opposite to the trend observed for succinic acid-coated soot (Figure 4(b)). Also, when soot aerosol is subjected to lower concentration of glutaric acid vapor (8.0×10^{11} molecule cm^{-3}), the aggregates shrink considerably, but only a small increase in the particle mass is detected. The striking inconsistency between

changes in the particle size and mass after coating can be explained by a partial loss of the glutaric acid coating during aerosol transport along the connecting tubing from the coating chamber to DMA2 and APM. Glutaric acid is substantially more volatile than succinic acid and its saturation vapor pressure at room temperature is high enough that a significant fraction of the coating can be lost from the particle surface by evaporation. For instance, Cruz and Pandis (2000) reported that partial losses of the pure glutaric acid led to uncertainties during aerosol deliquescence measurements. It is expected that the relative loss rate is inversely proportional to the particle size (Seinfeld and Pandis, 1998) and we confirmed this in evaporation rate experiments using TDMA with pure glutaric acid aerosol prepared by atomization of glutaric acid aqueous solution. During transport from the coating chamber to DMA2, glutaric acid particles with initial sizes 80–350 nm experienced a 45–11% mobility size decrease. For the smallest 50 nm glutaric acid particles evaporation was so efficient that the size decreased below the detection limit of our TDMA system (20 nm).

The high RH cycle while having a small effect on the mobility size, causes an unexpectedly significant promotion to the mass increase of coated soot particles. When the deliquescence point of glutaric acid at 83–99% RH (Prenni et al., 2001; Saxena and Hildemann, 1997) is reached, water condenses on the particle surface and dissolves glutaric acid, increasing the coating volume. Upon drying to 5% RH, a small fraction of water taken up at higher humidity remains trapped within the coating, leading to the observed mass increase. The particle size remains constant because the aqueous solution of glutaric acid fills up the void space within the aggregate between the primary carbon

spheres instead of forming a shell around the particle.

The effective density of soot particles increases significantly upon coating with glutaric acid as shown in Figure 7. Coated and heated soot is 1.5–3.0 times denser than fresh soot. Since the mass of particles first coated and then heated is similar to that of fresh soot, the increased effective density is caused by restructuring of the soot cores to a more compact morphology. A significant additional increase in the effective density of coated particles occurs upon exposure to high RH cycle. A distinct maximum of effective density observed for the processed soot at 80 nm arises because the smallest coated particles (d_{me} = 50 nm) have a higher relative coating evaporation rate and lose the coating faster than the larger particles. A similar trend has been reported in previous studies for the density of diesel exhaust particles (Maricq et al., 2000; Ahlvik et al., 1998).

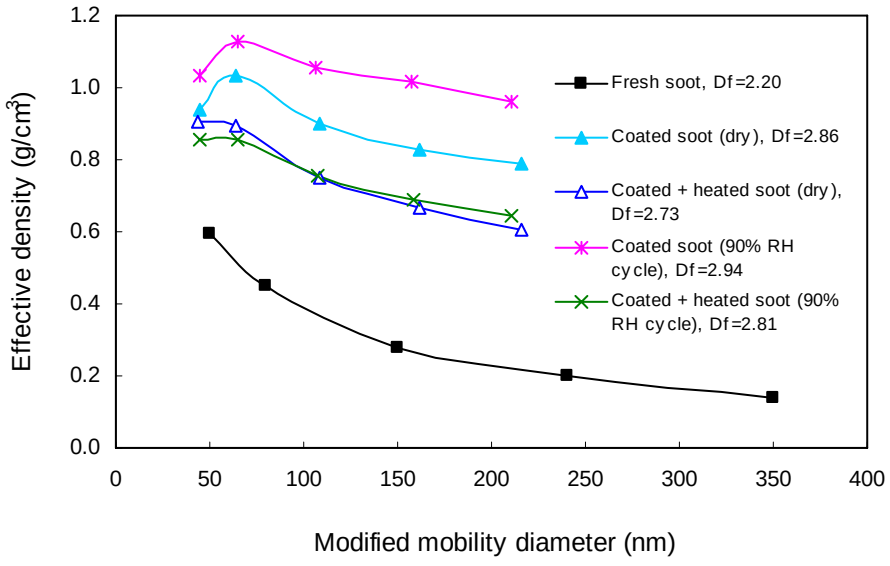

Figure 7. Effective densities of fresh and glutaric acid-coated soot particles as a function of processed mobility diameter. The fractal dimension (D_f) was obtained using equation (1).

The increase in particle mass and decrease in mobility size upon coating with glutaric acid are accompanied by an increase of the mass fractal dimension from 2.20 for fresh soot to 2.86 for coated soot under dry condition. For the coated soot exposed to high RH cycle, D_f increases to 2.94, confirming that the glutaric acid aqueous solution has filled up the voids in the aggregates when the acid deliquesced at high relative humidity. After the condensed acid is removed by the heater, the values of D_f decrease to 2.73 and 2.81 for dry and high RH cycle conditions, respectively. These values are significantly higher than those for fresh soot, indicating that the restructuring caused by glutaric acid coating is irreversible.

The difference of morphology behavior of soot agglomerates coated with succinic and glutaric acids can be depicted by a schematic diagram in Figure 8. When fresh soot aggregates are exposed to the succinic acid vapor, the coating is significant with growth of both particles mass and size, but no significant restructuring happens. For

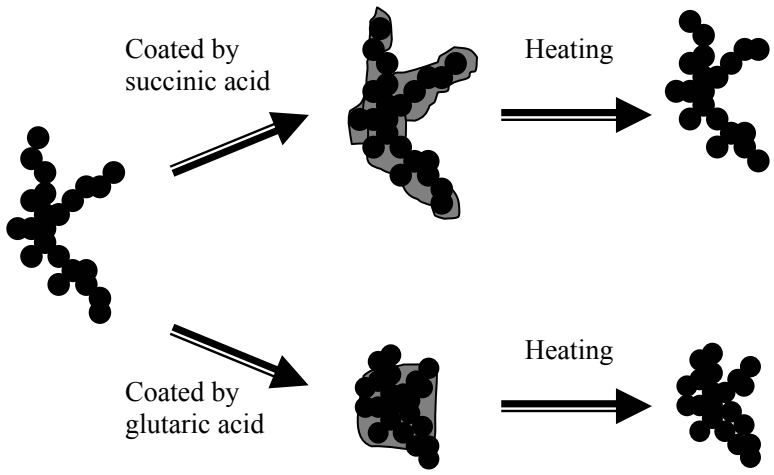

Figure 8. A schematic diagram showing the difference of morphology behaviors of soot aggregates with coatings of succinic and glutaric acids.

the soot aggregates exposed to glutaric acid vapor, the coatings leads to particles shrinking accompanying with particles mass increasing. The soot cores continue to restructure and become more compact with the additional 90% RH cycle.

In the case of liquid coatings, such as those composed of sulfuric acid (Zhang et al., 2008) and ozonolysis products of α-pinene (Saathoff et al., 2003), the force leading to compaction of agglomerates is the surface tension of the liquid that brings the primary particles into a closer configuration in order to minimize the surface of the liquid (Glasstetter et al., 1991). Once the contact region between the solid surfaces is replaced by a contact of liquid to liquid, the restructuring of the agglomerates can occur. The extent of restructuring induced by condensation depends on the liquid-solid interaction, i.e. the surface tensions of the condensing liquid and the solid (Topping et al., 2006). For instance, significant restructuring has been observed for hydrophobic butane-air flame soot exposed to subsaturated vapors of n-hexane and 2-propanol whereas water vapor yielded nearly no effect (Kütz and Schmidt-Ott, 1992). However, in the supersaturated environment even water vapor could promote restructuring when sufficient amount of liquid condensed onto the particle surface.

At first glance, the mechanism described above is inapplicable to succinic and glutaric acids since they are crystalline at room temperature. Glutaric acid molecule, containing five carbon atoms, has significantly lower melting temperature (99 °C) than succinic acid (188 °C), which contains only four carbon atoms. Lower melting temperature of glutaric acid is caused by the twisted molecular conformation in the crystal lattice due to the presence of an odd number of carbon atoms in its molecule.

Melting points of dicarboxylic acids show an alternating trend where the acids containing even number of carbon atoms exhibit systematically higher melting points compared to odd ones (Thallaid et al., 2000). A similar trend has also been observed for vapor pressures and sublimation enthalpies, where higher pressures and lower enthalpies correspond to less stable crystal structure of odd members (Bilde et al., 2003). Strained torsional conformation of glutaric acid in solid state and the associated excess energy as compared to succinic acid may lead to stronger interaction of glutaric acid with the soot surface. Because of this interaction, formation of a "subcooled" liquid layer rather then crystal might be more thermodynamically or kinetically feasible when the first few monolayers of glutaric acid condense on the soot surface. This quasi-liquid layer can promote the aggregate collapse even under dry conditions as observed in the present study and reported earlier by Mikhailov et al. (2006). Another indication of a strong interaction between glutaric acid and soot comes from our recent heterogeneous uptake study where desorption of glutaric acid (Levitt et al., 2007) from the soot surface was found to be significantly slower than desorption of succinic acid (unpublished data).

3.2. Inherent material Density and Dynamic Shape Factor

For the agglomerated soot particles, the measured effective density is typically significantly lower than the inherent material density. To estimate the inherent material density of coated soot, the mass fraction of soot, f_{soot}, and acid coating, f_{acid}, were first determined from APM measurements. Using the inherent material densities of pure soot, ρ_{soot} = 1.77 g cm^{-3} (Park et al., 2004b), $\rho_{succinic\ acid}$ = 1.55 g cm^{-3} and $\rho_{glutaric\ acid}$ = 1.43 g cm^{-3} (Peng et al., 2001), the inherent material density of the coated soot particles ($\rho_{coated,}$

$_{inherent}$) can be expressed as:

$$\rho_{inherent} = \frac{1}{\frac{f_{acid}}{\rho_{acid}} + \frac{f_{soot}}{\rho_{soot}}}. \quad (7)$$

The calculated values of inherent material densities, 1.64–1.71 g cm^{-3}, are significantly higher than the measured effective densities, suggesting the existence of the internal voids in the compacted soot.

Based on the inherent material density, the volume equivalent diameter (d_{ve}) can be determined, which is defined as the diameter of a spherical particle having the same volume as the irregularly shaped particle. The volume equivalent diameter can further be used to calculate the dynamic shape factor, χ, which is a measure of the increased drag experienced by an irregular particle in comparison to a sphere of equivalent volume moving at the same speed. The general expression for the dynamic shape factor is (DeCarlo et al., 2004)

$$\chi = \frac{d_{me}}{d_{ve}} \bullet \frac{C_{ve}}{C_{me}}, \quad (8)$$

where C_{ve} and C_{me} are the Cunningham slip correction factors calculated by d_{ve} and d_{me}, respectively. The dynamic shape factor is almost always greater than one for irregular particles and equal to one for spheres.

Figure 9 compares the size-dependent dynamic shape factors for fresh soot with those for soot processed by condensation of glutaric and succinic acids. For fresh soot, χ increases from 2.2 to 4.7 with particle mobility diameter increasing from 50 to 350 nm.

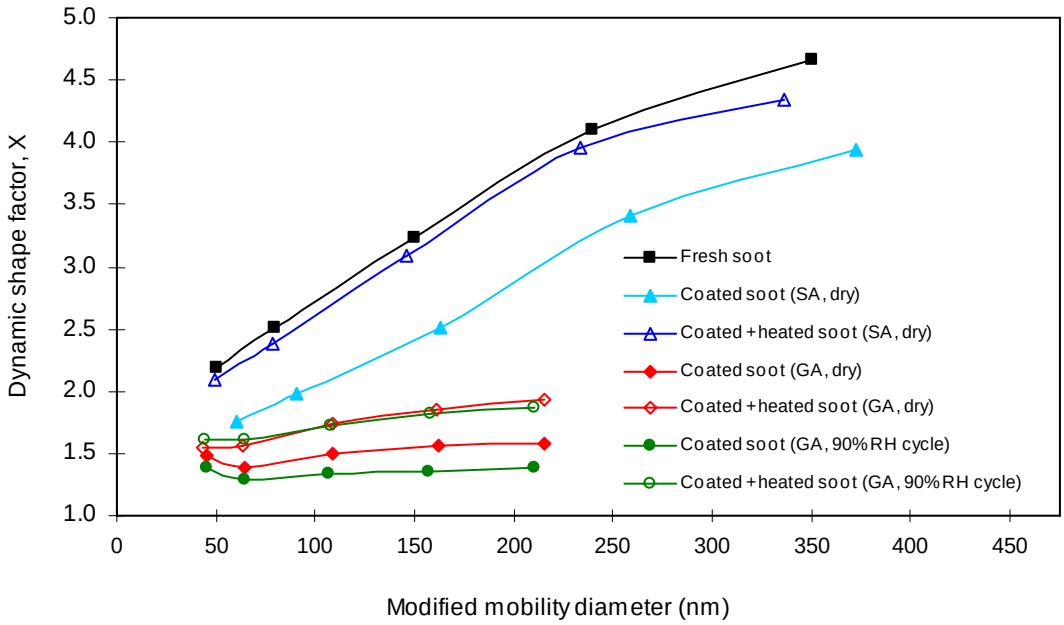

Figure 9. The dynamic shape factors as a function of mobility diameter for fresh and coated soot (SA = succinic acid, GA = glutaric acid).

The dynamic shape factor for fresh soot is higher than that measured for diesel soot (Park et al., 2004a). Coating the soot aggregates with organic acids lowers χ to 1.5–1.8 because the condensed material fills up the voids, reducing the drug. The dynamic shape factors of soot particles coated by glutaric acid are significantly lower than those for soot coated by succinic acid, in good agreement with our fractal dimension analysis. For soot coated with glutaric acid, the dynamic shape factor decreases to 1.29–1.38 after exposure to high RH cycle. When the condensed glutaric acid is removed by heating, χ increases insignificantly, indicating a substantial restructuring of the soot cores. However, heating the soot coated with succinic acid restores χ to values close to those measured for fresh soot because no restructuring has occurred.

3.3. Atmospheric Implications

Our measurements show that soot particles exposed to glutaric acid vapor experience significant changes in morphology and become more compact and dense whereas succinic acid does not promote the restructuring. Soot may acquire a significant fraction of dicarboxylic acid coating during atmospheric aging and the extent of restructuring is strongly dependent on the type and mass fraction of acid and initial particle size. Under high humidity conditions, soot with hydrophilic coating can experience an additional compaction.

Hygroscopic soot internally mixed with glutaric acid deliquesces at subsaturated RH conditions and hence can play a role in haze formation. Deliquesced particles exhibit stronger light scattering and absorption (Mikhailov et al., 2006), resulting in visibility reduction and altered direct climate forcing. Pure glutaric acid particles have been previously shown to readily activate to cloud droplets at supersaturations below 0.3% (Prenni et al., 2001). Thus, glutaric acid-coated soot can affect cloud formation and force climate indirectly. Increased hydrophilicity of aged soot can shorten its lifetime in the atmosphere because hydrophilic soot particles can be effectively removed by wet scavenging. Also, the changes in hygroscopicity, morphology, and effective density of soot aerosol during atmospheric aging can modify its deposition in respiratory system and are likely relevant to human health.

4. ENHANCED OPTICAL PROPERTIES OF SOOT PARTICLES

4.1. Optical Properties of Fresh and Coated Soot Aggregates

The evolution of the optical cross-sections for soot particles with initial diameter D_p = 245 nm processed by glutaric acid and heating is depicted in Figure 10. For fresh soot, scattering is weak and the extinction is dominated by absorption, resulting in a single scattering albedo ω, i.e. the ratio of scattering to exaction, as low as 0.09. The fresh soot consists of small primary spherules combined into branched aggregates with a low effective density and a relatively open structure, scattering by aggregates is weak even though their mobility diameters are comparable with the light wavelength. As mentioned previously (Xue et al., 2008a), the hydrophilic particles were generated by coating with glutaric acid vapor onto the fresh soot. The size-dependent mass ratio of glutaric acid to

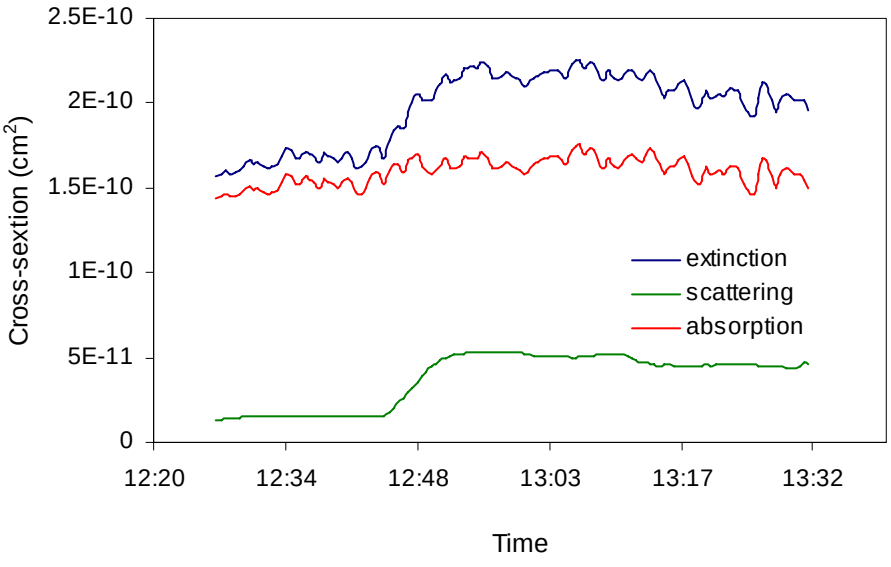

Figure 10. Temporal profile of the extinction, scattering, and absorption cross-sections of soot aerosol (λ = 532 nm) after exposure to the glutaric acid vapor (8.5×10^{12} molecule cm-3). The initial particle mobility diameter is 245 nm and relative humidity is 5%.

soot was measured in the range of 0.22–0.31 in dry condition (5% RH). Our mass-mobility relationship results have shown that the fresh soot aggregate restructured by collapsing the branched structures and forming a more dense globular shape (Xue et al., 2008a), which also leads a significant change in the optical properties. As depicted in Figure 10, light extinction and scattering increase by a factor of 1.15 and 3.13, respectively. The value of single scattering albedo increases from 0.09 for fresh soot to 0.24 for coated soot by glutaric acid. The scattering cross section values were still surprising higher than the initial values of fresh soot even the coatings were remove by heating, indicating a solid increasing of scattering by morphology changes.

The amplification of optical properties for soot particles with initial diameters of 155, 245, and 320 nm exposure to glutaric and succinic acids are presented in Figures 11

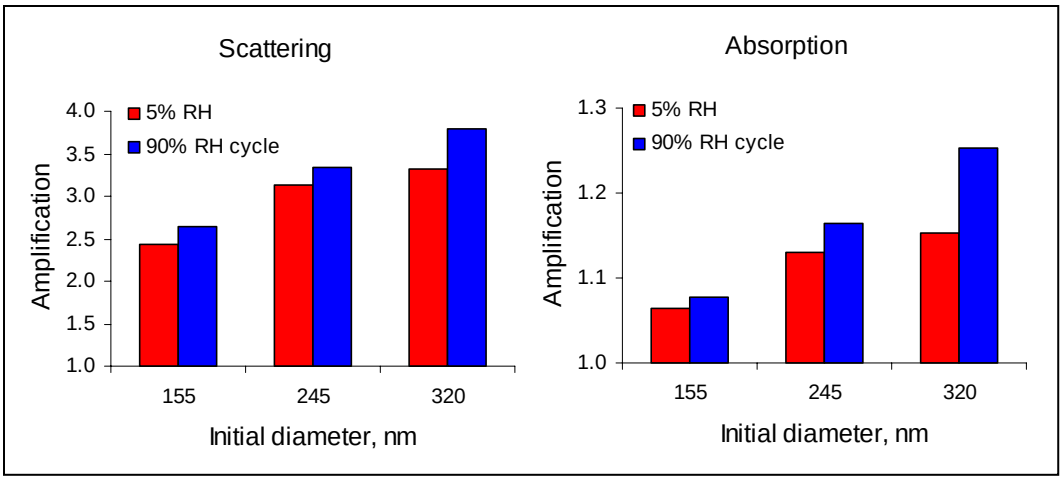

Figure 11. Amplification factors of soot scattering, and absorption cross-sections (λ = 532 nm) after exposure of aerosol to the glutaric acid vapor (8.5×10^{12} molecule cm^{-3}) at 5% RH or an additional 90% RH cycle. The initial (uncoated) particle mobility diameters are 155, 245, and 320 nm.

and 12, respectively. An additional 90% RH cycle (coated soot was exposed to 90% RH then dried to 5% RH) are supposed to the further enhancement on optical properties by excess water vapor. After exposure of soot to glutaric acid, the mass fraction of glutaric acid were 0.18–0.24 in 5% RH and 0.27–0.33 with 90% RH cycle (Xue et al., 2008a), and the scattering cross-section increase significantly by 2.44–3.32 times (5% RH) and 2.64–3.79 times (90% RH cycle). The enhancement of Csca is size-dependent with large soot particles get more enhancement than the small particles. Single scattering albedo (SSA) of fresh soot particles also gets amplified with the same trend. The 90% RH cycle only show a limited further enhancement than that in 5% RH condition. These are in full agreement with our mass-mobility relationship measurements, which suggested that the soot particles morphology restructured to more dense shape upon coating with glutaric acid, and the large particles shrunk more. The shrinking factors of mobility diameter in 5% RH and 90% RH cycle are comparable, which are also in good agreement with the current comparable optical enhancement results.

Absorption always increase when internal mixing with sulfuric acid occurs but the observed enhancement is smaller than scattering. For the 320 nm soot particle, the amplify factor for absorption is about 1.25 exposure to glutaric acid with 90% RH cycle. Mikhailov et al. (2006) report that glutaric acid does not absorb radiation in visible spectrum; therefore an increase in shell thickness leads to an increase of the scattering cross section, extinction cross section and SSA. But the absorption cross section tends to increase after being coated with a glutaric acid shell.

For soot exposed to succinic acid (4.4×10^{13} molecule cm^{-3}, acid coating mass

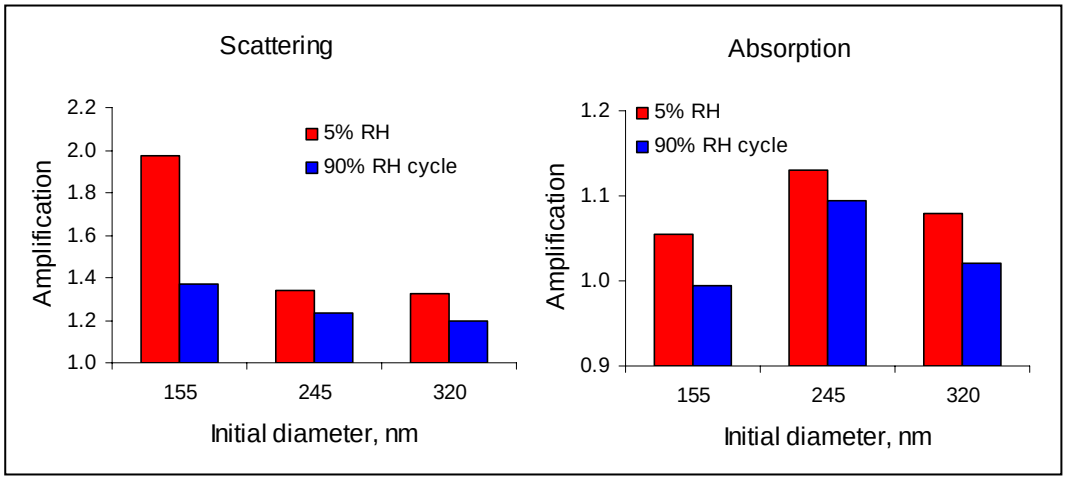

Figure 12. Amplification factors of soot scattering, and absorption cross-sections (λ = 532 nm) after exposure of aerosol to the succinic acid vapor (4.4×10^{13} molecule cm^{-3}) at 5% RH or an additional 90% RH cycle. The initial (uncoated) particle mobility diameters are 155, 245, and 320 nm.

fraction is in the range of 0.44–0.35), the scattering cross-section increases for all particle sizes and at 5% RH becomes 1.32–1.97 times larger than that of fresh soot (Figure 12). However, no visible increase of SSA was observed. The scattering enhancement is size-dependent with decreasing with particle size, which shows an opposite trend to the coated soot particle with glutaric acid. This opposite trend is in good agreement with the morphology results, which show that fresh soot particles getting shrunk upon coating with glutaric acid, but growing upon coating with succinic acid and small particles get higher growth factor in mobility diameter. The absorption cross-section, on the other hand, only a very small increase in the range of 1.05–1.13 happens. Also, both the absorption and scattering do not increase with 90% RH cycle

since the 90% RH is still below the succnic acid's deliquescence point of 99% RH (Saxena and Hildemann, 1997; Prenni et al., 2001) and is not likely exhibit hygroscopic growth. Since no significantly restructuring happens to soot aggregates upon coating with succinic acid, the enhancement of both scattering and absorption are likely contributed by transparent material condenses on the surface of soot aggregates and hence the particle size growth. Bond et al. (2006) found that depositing a shell of non-absorbing material around a pure light-absorbing carbon (LAC) particle can increase the absorption of the pure absorbing particle using a concentric-shell-and-core model. In laboratory experiments, Schnaiter et al. (2003) observed amplification of about 1.35 for soot particles thinly coated with secondary organic aerosol. Later experiments producing thicker coatings of organic material showed a maximum amplification of 1.8–2.1 (Schnaiter et al., 2005).

4.2. Enhancement Mechanism

The formation of a transparent shell and restructuring of the soot aggregates can both contribute to the increased light scattering and absorption by coated soot particles. To distinguish between these two effects, we measured the change in scattering and absorption by soot subjected to a combination of coating and heating.

As shown in Figure 13, heating the fresh (uncoated) soot particles to 200 °C has no effect on scattering, but leads to a 1.04–1.14 fold increase in absorption, with smaller values for larger particle sizes. This effect is explainable since absorption by aggregates is increased by about 1.3 times over individual primary spherules (Fuller et al., 1999) and this factor can be completely or partially lost when particles are thinly coated with

non-absorbing material. If fresh soot aggregates carry a very thin layer of condensed organics, heating the soot will remove some or all of the coating, resulting in an increased absorption. The amount of the coated organic material is low for soot used in our

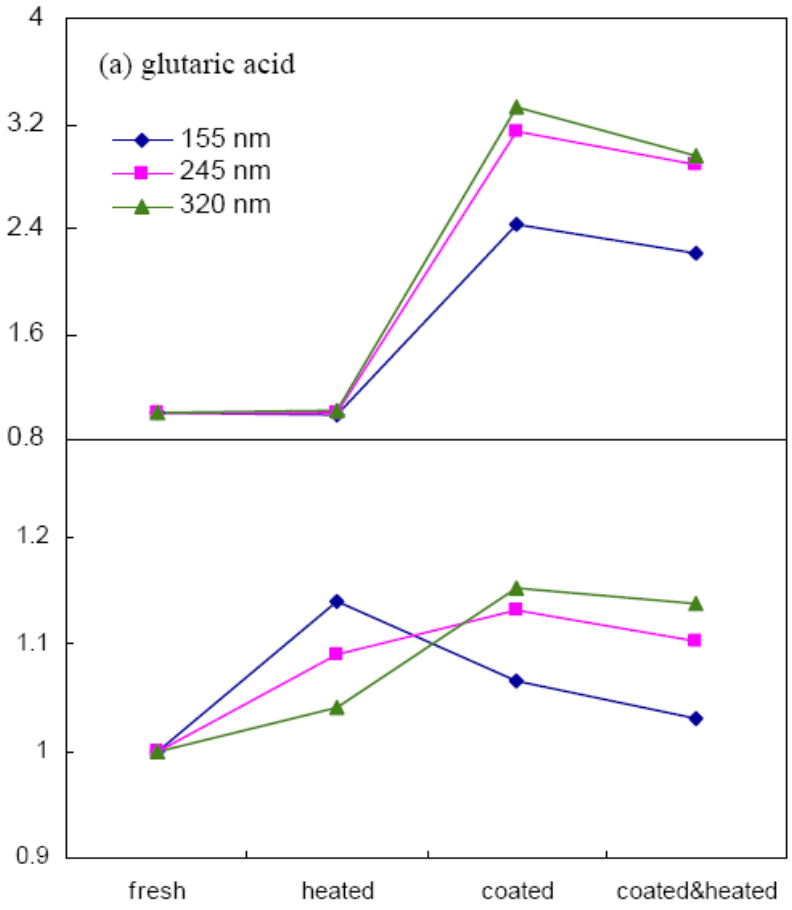

Figure 13. Variations in light scattering and absorption (λ = 532 nm) by soot agglomerates subjected to different types of processing (a) exposed to the glutaric acid and (b) exposed to the succinic acid. "Fresh" stands for uncoated soot aerosol, "heated" for soot aerosol that is heated to 200 °C, "coated" for soot aerosol that is exposed to acid vapor, "coated&heated" for soot aerosol that is exposed to acid vapor and subsequently heated to 200°C. The initial (uncoated) soot particle mobility diameters are 155, 245, and 320 nm and relative humidity is 5% RH.

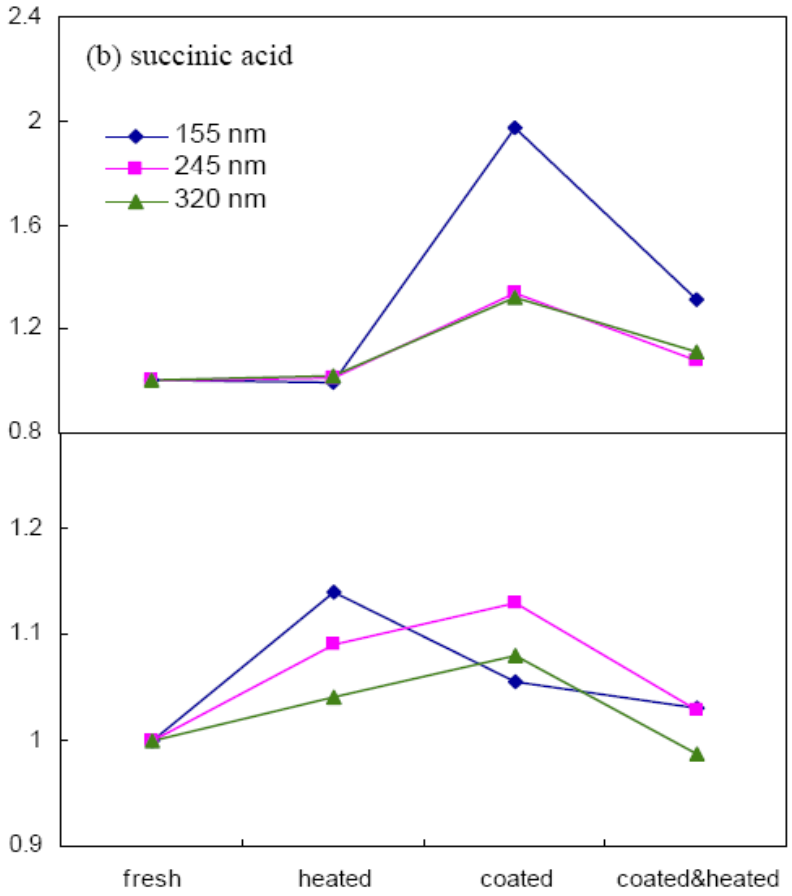

Figure 13. Continued.

experiments because scattering is not affected by heating. This is in agreement with the results of our DMA-APM measurements indicating that the mass ratio of heated to fresh soot is 1.00±0.03 (Xue et al., 2008a).

Exposure of soot aerosol to glutaric acid results in a strong enhancement of light scattering (Figure 13(a)). Heating the coated soot particles to remove sulfuric acid reduces the enhancement. However, scattering by coated and heated soot is still significantly higher than scattering by fresh soot. Since the mass of particles that are first coated and

then heated is similar to the mass of fresh soot, the increased scattering is caused entirely by irreversible restructuring of the soot cores to a more compact form. Primary spherules in compacted aggregates interact collectively with electromagnetic wave, leading to stronger scattering. Thus, transparent coating affects scattering both directly, through increased particle volume, and indirectly, by changing the soot core morphology. As for the soot particles exposed to succinic acid, no significant restructuring was observed (Xue et al., 2008a). The increased scattering is caused entirely by the formation of the transparent shell over the surface of the fresh soot particle (Figure 13(b)). The scattering of small particle increased more than big particle upon coating with succinic acid because of the thicker coating shell. A small enhancement of scattering was observed even the coated succinic acid was removed by heating, which was supposed to the slightly morphology change during succinic acid melt and evaporate in heater.

The restructuring is also a major contributor to enhancement of light absorption by soot. Figure 13(a) shows that for large soot particles, enhancement caused by glutaric acid coating is reduced insignificantly by subsequent removal of sulfuric acid through heating. Soot particles with initial diameter of 155 nm, however, show smaller increase in absorption after exposure to sulfuric acid, and subsequent heating of these particles reduces absorption to a lower value. The different behavior for large and small aggregates is explained by the combined effects of restructuring on the interaction between primary spherules and increased effective density of the soot cores caused by processing (Khalizov et al., 2008a). The net result of coating and heating in the case of small particles corresponds to nearly complete cancellation between enhancement and shielding caused

by restructuring. Larger particles, having lower initial density, experience stronger relative compaction when coated and heated, but the final core densities of 0.67 and 0.58 g cm^{-3} for 245 nm and 320 nm particles, respectively, are lower than for 155 nm particles. Therefore, the enhancement factor dominates over the shielding, and the absorption cross-section remains above that for fresh soot. Absorption of soot particles coated with succinic acid was also enhanced to a small extent, and subsequent heating of these particles reduces absorption to the values slightly over that for fresh soot. Theoretical model shows that absorption is always increased when soot mixes with nonabsorbing materials and amplification is slightly sensitive to chosen particle size (Bond et al., 2006). Our previous studies show that the optical enhancement may also depends on the initial size and morphology of fresh soot aggregates (density, fractal dimension, and diameter of primary spherules) and the properties of the coating material. The complex variation in morphology of soot agglomerates are critical to the optical properties of atmospheric carbonaceous particles, which should be taken into account accurately in the future model calculations.

The term of mass-specific absorption cross-sections (MAC) is commonly used to describe the absolute magnitude of atmospheric absorption. The variation in the reported values of MAC of soot represents one of the major factors leading to large uncertainties in the evaluation of the atmospheric optical effects. Bond and Bergstrom (2005) reviewed 21 measurements and suggested a value of 7.5±1.2 m^2 g^{-1} for the MAC of fresh light-absorbing carbon. Ambient values of MAC in polluted regions tend to exhibit a mode around 9–12 m^2 g^{-1}. We have reported the MAC values range from 6.1 to 8.8 m^2 g^{-1}

for fresh soot aerosol at 5% RH, and 12.6 m^2 g^{-1} upon internally mixed with H_2SO_4 vapor at 80% RH (Khalizov et al., 2008a). In this study, we measured the optical properties of well-characterized fresh and internally mixed soot aerosol, and combined with the previous mass-mobility results to determine the MAC values, which are shown in Table 2.

Table 2. Mass-specific absorption cross-sections of soot aerosol (λ = 532 nm) before and after exposure to glutaric aicd and succinic acid vapor

RH	Mass-specific absorption cross-section, m^2 g^{-1}					
	Succinic acid, 4.4×10^{13} molecules cm^{-3}					
	D_p = 155 nm		D_p = 245 nm		D_p = 320 nm	
	fresh	coated	Fresh	coated	fresh	coated
5%	7.4±0.7	7.9±1.6	7.7±1.6	8.9±1.7	8.6±2.0	9±1.5
90% Cycle	7.7±0.3	7.7±0.9	7.9±1.5	8.8±1.1	8.8±1.2	8.9±1.1
	Glutaric acid, 8.5×10^{12} molecules cm^{-3}					
5%	7.2±0.8	7.7±0.9	7.7±0.3	9.0±0.6	8.9±1.0	10.5±0.7
90% Cycle	7.7±0.3	8.1±1.0	7.8±0.4	9.3±0.9	8.6±1.4	10.8±3.8

The size-dependent MAC values are determined in the range of 7.2–8.9 m^2 g^{-1} for the fresh soot particles, which are in good agreement with the previous results. MAC values of soot particles are enhanced by ~25% due to coating with dicarboxylic acids. During a particle's atmospheric lifetime, MAC value may increase due to coating and decrease due to particle coagulation and aggregate collapse (Bond and Bergstrom, 2005).

4.3. Atmospheric Implications

Our results imply that in polluted region, air visibility can be considerably reduced due to the formation of haze and polluted clouds by condensation of organic acid and saturated water vapor on hygroscopic soot nuclei. We provide the direct laboratory

evidence for the amplification of scattering and absorption by the internally mixed soot-organics agglomerates. Particles made of pure glutaric acid readily activated as cloud droplets at <0.3% supersaturation and thus play a role in haze formation and visibility reduction (Prenni et al., 2001). Succinic acid particles, on the other hand, are not likely to exhibit hygroscopic growth under most humidity conditions because the high deliquescence point, but they may play a role in developing haze particles after they have been processed by cloud. In a previous study (Zhang et al., 2008), we have reported that aged soot with H_2SO_4 can activate readily to serve as cloud condensation nuclei (CCN) under various cloud conditions. And the aerosol optical depth (visibility) of the aged soot in polluted air is strongly correlated with RH.

This study suggests that the optical properties of black carbon are altered even if non-absorbing materials are mixed with black carbon in model studies. In case of thin layers, However, the coated sphere optical model is only a rough approximation and may lead to significantly errors in the calculated optical properties and hence the direct radiative forcing (Schnaiter et al., 2005). We provided laboratory evidence of amplification factors on the basis of soot particle core size, amount and species of mixing materials, which results in a better agreement between modeled and observed optical properties. These results will result in parameterization of aerosol microphysical processes and substantially improve the climate models predictive capabilities.

The coatings with dicarboxylic acids on soot aerosol lead to observed enhancement of scattering and absorption, as well as a limited increase of single scattering albedo. Therefore, these results may have the opposing effects of adding energy to the

atmosphere and reducing it at the surface. The uncertainty in understanding climate change also arises from the effects of soot aerosol on cloud formation and subsequent indirect radiative forcing. Field investigations (Ramanathan et al., 2001) suggest that the absorption by aerosols consisting of organics and element black carbon can explain as much as 4-5 W/m^2 of the excess absorption. The amplified absorption of internally mixed soot aerosol implies the reduction of photolysis rates and a lower ground level ozone concentration during heavy air pollution period (Li et al., 2005). Enhanced light absorption and scattering can stabilize the atmosphere because of cooling at the earth surface and warming aloft. This will have an important feedback on air quality and cloud dynamics (Fan et al., 2008). Nenes et al. (2002) suggest that the sign of the climatic feedback from black carbon heating on cloud microphysics can be either positive or negative and the overall black carbon influence on climate are more complex than the previously thought.

5. CONCLUSIONS

A series of experiments was performed in which the soot particles generated in the propane/air flame was alternately coated with glutaric and succinic acids, respectively. Particles processing involved condensation of the two dicarboxylic acids, various humid conditions and evaporation of the acids by heating. Simultaneous measurements with TDMA and DMA-APM enabled us the particle mass, mobility size, volume, effective density, fractal dimension, fractional composition, and dynamic shape factor.

Coatings with gultaric acid result in significant changes in soot particle morphology by restructuring and make particles more compact and dense, but succinic acid does not show the restructuring promotion. The size-dependent mass growth factors for coatings with succinic and glutaric acids show the opposite trends because the strong evaporation of glutaric acid, particularly on the small particles.

For given soot source, the extent of restructuring is strongly dependent on the type and mass fraction of acid, as well as the humid conditions and particle size. Soot with a hydrophilic coating experiences an additional restructuring to a more compact core at high RH. The voids in the coated particles also may be an important factor to characterize the extent of transformation to spherical particles. Hygroscopic coating and restructuring may happen to soot particles with other common compounds e.g. sulfuric acid in the atmosphere. Understanding the atmospheric processing of soot particles is crucial to better evaluate the global direct and indirect effects of soot aerosols.

In this paper, I have studied the extinction and absorption properties of the well-characterized soot particles from a propane diffusion flame upon atmospheric

processing. Internally mixed soot aerosol with a known morphology and mixing state is produced by exposure to gaseous glutaric and succinic acid, respectively. Coated airborne soot particles are subjected to controlled humidity environment and the light extinction, scattering, and absorption cross-sections at 532 nm are determined using a combination of a cavity ring-down spectrometer and an integrating nephelometer.

It was suggested that light scattering and absorption cross-sections of fresh soot were significantly enhanced with the factors of ~3.8 and ~1.25 respectively upon internally mixing with glutaric acid. The irreversible restructuring and transparent coating of soot aggregates caused by condensation of glutaric acid and water can alter both scattering and absorption. Enhancement of optical properties is size-dependent with increasing with the initial size of soot aggregates. For the soot particles internally mixed with succinic acid, the amplification factor of scattering were observed in the range of 1.2–1.7 at 5% RH and small increasing was observed to light absorption. Coatings with organic acids also result in the enhancement of single scattering albedo and mass-specific absorption cross-sections of fresh soot aggregates. Our results provide the laboratory evidence for thinly coated soot aggregates, i.e., the Mie theory calculations on a shell-and-core model is not appropriate in this case. These enhanced optical values indicate that coatings on soot aerosol particles significantly impact soot's role in regional visibility and air quality and global climate change.

REFERENCES

Ackerman, A. S., Toon, O. B., Stevens, D. E., Heymsfield, A. J., Ramanathan, V., & Welton, E. J. (2000). Reduction of tropical cloudiness by soot. *Science*, *288*, 1042–1047.

Ahlvik, P., Ntziachristos, L., Keskinen, J., & Virtanen, A. (1998). *Real time measurements of diesel particle size distribution with an electrical low pressure impactor*. SAE Technical Paper, No. 980410.

Bilde, M., Svenningsson, B., Mönster, J., & Rosenorn, T. (2003). Even-odd alternation of evaporation rates and vapor pressures of C3-C9 dicarboxylic acid aerosol. *Environmental Science and Technology*, *35*, 1371–1378.

Bond, T. C., & Bergstrom, R. W. (2005). Light absorption by carbonaceous particles: An investigative review. *Aerosol Science and Technology*, *39*, 1–41.

Bond, T. C., Habib, G., & Bergstrom, R. W. (2006). Limitations in the enhancement of visible light absorption due to mixing state. *Journal of Geophysical Research*, *111*(D20211), doi:10.1029/2006JD007315.

Bond, T. C., Streets, D. G., Yarber, K. F., Nelson, S. M., Woo, J. H., & Klimont, Z. (2004). A technology-based global inventory of black and organic carbon emissions from combustion. *Journal of Geophysical Research*, *109*, D14203, doi:10.1029/2003JD003697.

Cruz, C. N., & Pandis, S. N. (2000). Deliquescence and hygroscopic growth of mixed inorganic-organic atmospheric aerosol. *Environmental Science and Technology*, *34*,

4313–4319.

DeCarlo, P. F., Slowik, J. G., Worsnop, D. R., Davidovits, P., & Jimenez, J. L. (2004). Particle morphology and density characterization by combined mobility and aerodynamic diameter measurements. Part 1: Theory. *Aerosol Science and Technology*, *38*, 1185–1205.

Ehara, K., Hagwood, C., & Coakley, K. J. (1996). Novel method to classify aerosol particles according to their mass-to-charge ratio: Aerosol particle mass analyzer. *Journal of Aerosol Science*, *27*, 217–234.

Fan, J., Zhang, R., Tao, W., & Mohr, K. I. (2008). Effects of aerosol optical properties on deep convective clouds and radiative forcing. *Journal of Geophysical Research*, *113*(D08209), doi:10.1029/2007JD009257.

Fuller, K. A., Malm, W, C., & Kreidenweis, S. M. (1999). Effects of mixing on extinction by carbonaceous particles. *Journal of Geophysical Research*, *104*(D13), 15941–15954.

Geller, M., Biswas, S., & Sioutas, C. (2006). Determination of particle effective density in urban environments with a differential mobility analyzer and aerosol particle mass analyzer. *Aerosol Science and Technology*, *40*, 709–723.

Glasstetter, R., Ricketts, C. I., & Wilhelm, J. G., (1991). Towards modeling the meniscus geometry and volume of capillary water between two contacting microspheres in moistair. *Journal of Aerosol Science*, *22*, S195–198.

Huang, P. F., Turpin, B. J., Pipho, M. J., Kittelson, D. B., & McMurry, P. H. (1994). Effects of water condensation and evaporation on diesel chain-agglomerate

morphology. *Journal of Aerosol Science*, *25*, 447–459.

Intergovernmental Panel on Climate Change (IPCC) (2007). *IPCC Technical Paper on Climate Change and Water*. Cambridge: Cambridge University Press.

Jacobson, M. Z. (2001). Strong radiative heating due to the mixing state of black carbon in atmospheric aerosols. *Nature*, *409*, 695–697.

Kaufman, Y. J., Tanre, D., & Boucher, O. (2002). A satellite view of aerosols in the climate system. *Nature*, *419*, 215–223.

Khalizov, A. F., Xue, H., & Zhang, R. (2008a). Enhanced light absorption and scattering by carbon soot aerosols internally mixed with sulfuric acid. *Journal of Physical Chemistry*, accepted.

Khalizov, A. F., Zhang, R., Zhang, D., Xue, H., Pagels, J., & McMurry, P. H. (2008b). Formation of highly hygroscopic aerosols upon internal mixing of airborne soot particles with sulfuric acid vapor. *Journal of Geophysical Research*, accepted.

Kütz, S., & Schmidt-Ott, A. (1992). Characterization of agglomerates by condensation-induced restructuring. *Journal of Aerosol Science*, *23*, S357–360.

Levitt, N. P., Zhang, R., Xue, H., & Chen, J. (2007). Heterogeneous chemistry of organic acids on soot surfaces. *Journal of Physical Chemistry*, *111*, 4804–4814.

Li, G., Zhang, R., Fan, J., & Tie, X. (2005). Impacts of black carbon aerosol on photolysis and ozone. *Journal of Geophysical Research*, *110*(D23206), doi:10.1029/2005JD005898.

Maricq, M. M., Podsiadlik, D. H., & Chase, R. E. (2000). Size distributions of motor vehicle exhaust PM: A comparison between ELPI and SMPS measurements. *Aerosol*

Science and Technology, *33*, 239–260.

Maricq, M. M., & Xu, N. (2004). The effective density and dimension of soot particles from premixed flames and motor vehicle exhaust. *Journal of Aerosol Science*, *35*, 1251–1274.

McMurry, P. H., Wang, X., Park, K., & Ehara, K. (2002). The relationship between mass and mobility for atmospheric particles: A new technique for measuring particle density. *Aerosol Science and Technology*, *36*, 227–238.

Mikhailov, E. F., Vlasenko, S. S., Podgorny, I. A., Ramanathan, V., & Corrigan, C. E. (2006). Optical properties of soot-water drop agglomerates: An experimental study. *Journal of Geophysical Research*, *111*, D07209, doi:10.1029/2005JD006389.

Mönster, J., Rosenörn, T., Svenningsson, B., & Bilde, M. (2004). Evaporation of methyl- and dimethyl-substituted malonic, succinic, glutaric and adipic acid particles at ambient temperatures. *Journal of Aerosol Science*, *35*, 1453–1465.

Nenes, A., Conant, W. C., & Seinfeld, J. H. (2002). Black carbon radiative heating effects on cloud microphysics and implications for the aerosol indirect effect 2. Cloud microphysics. *Journal of Geophysical Research*, *107*(D21), doi:10.1029/2002JD002101.

Pagels, J., Khalizov, A. F., Emery, M., McMurry P. H., & Zhang, R. (2008). Processing of soot by controlled sulphuric acid and water condensation–mass and mobility relationship. *Aerosol Science and Technology*, submitted.

Park, K., Cao, F., Kittelson, D. B., & McMurry, P. H. (2003). Relationship between particle mass and mobility for diesel exhaust particles. *Environmental Science and*

Technology, *37*, 577–583.

Park, K., Kittelson, D. B., & McMurry P. H. (2004a). Structural properties of diesel exhaust particles measured by transmission electron microscopy (TEM): Relationships to particle mass and mobility. *Aerosol Science and Technology*, *38*, 881–889.

Park, K., Kittelson, D. B., Zachariah, M. R., & Mcmurry, P. H. (2004b). Measurement of inherent material density of nanoparticle agglomerates. *Journal of Nanoparticle Research*, *6*, 267–272.

Peng, C., Chan, M. N., & Chan, C. K. (2001). The hygroscopic properties of dicarboxylic and multifunctional acids: Measurements and UNIFAC predictions. *Environmental Science and Technology*, *35*, 4495–4501.

Penner, J. E., Eddleman, H., & Novakov, T. (1993). Towards the development of a global inventory for black carbon emissions. *Atmospheric Environment*, *27*, 1277–1295.

Prenni, A. J., DeMott, P. J., Kreidenweis, S. M., Sherman, D. E., Russell, L. M., & Ming, Y. (2001). The effects of low molecular weight dicarboxylic acids on cloud formation. *Journal of Physical Chemistry*, *105*, 11240–11248.

Ramanathan, V., & Carmichael, G. (2008). Global and regional climate changes due to black carbon. *Nature Geoscience*, *1*, 221–227.

Ramanathan, V., Crutzen, P. J., Kiehl, J. T., & Rosenfeld, D. (2001). Aerosols, climate, and the hydrological cycle. *Science*, *294*, 2119–2124.

Saathoff, H., Naumann, K. H., Schnaiter, M., Schock, W., Mohler, O., Schurath, U., Weingartner, E., Gysel, M., & Baltensperger, U. (2003). Coating of soot and

$(NH_4)_2SO_4$ particles by ozonolysis products of α-pinene. *Journal of Aerosol Science*, *34*, 1297–1321.

Santoro, R. J., Semerjian, H. G., & Dobbins, R. A. (1983). Soot particle measurement in diffusion flames. *Combustion and Flame*, *51*, 203–218.

Saxena, P., & Hildemann, L. M. (1996). Water-soluble organics in atmospheric particles: A critical review of the literature and application of thermodynamics to identify candidate compounds. *Journal of Atmospheric Chemistry*, *24*, 57–109.

Saxena, P., & Hildemann, L.M. (1997). Water absorption by organics: Survey of laboratory evidence and evaluation of UNIFAC for estimating water activity. *Environmental Science and Technology*, *31*, 3318–3324.

Schnaiter, M., Horvath, H., Möhler, O., Naumann, K.-H., Saathoff, H., & Schöck, O. (2003). UV-VIS-NIR spectral optical properties of soot and soot-containing aerosols. *Journal of Aerosol Science*, *34*, 1421–1444.

Schnaiter, M., Linke, C., Möhler, O., Naumann, K.-H., Saathoff, H., Wagner, R., Schurath, U., & Wehner, B. (2005). Absorption amplification of black carbon internally mixed with secondary organic aerosol. *Journal of Geophysical Research*, *110*(D19204), doi:10.1029/2005JD006046.

Schwarz, J. P., Spackman, J. R., Fahey, D. W., Gao, R. S., Lohmann, U., Stier, P., Watts, L. A., Thomson, D. S., Lack, D. A., Pfister, L., Mahoney, M. J., Baumgardner, D., Wilson, J. C., & Reeves, J. M. J. (2008). Coatings and their enhancement of black carbon light absorption in the tropical atmosphere. *Journal of Geophysical Research*, *113*(D03203), doi:10.1029/2007JD009042.

Seinfeld, J. H., & Pandis, S. N (1998). *Atmospheric chemistry and physics: From air pollution to climate change*. New York: John Wiley.

Shiraiwa, M., Kondo, Y., Moteki, N., Takegawa, N., Miyazaki, Y., & Blake, D. R. (2007). Evolution of mixing state of black carbon in polluted air from Tokyo. *Geophysical Research Letters*, *34*, L16803, doi:10.1029/2007GL029819.

Slowik, J. G., Stainken, K., Davidovits P., Williams, L. R., Jayne, J. T., Kolb, C. E., Worsnop, D. R., Rudich, Y., DeCarlo, P. F., & Jimenez, J. L. (2004). Particle morphology and density characterization by combined mobility and aerodynamic diameter measurements. Part 2: Application to combustion-generated soot aerosols as a function of fuel equicalence ratio. *Aerosol Science and Technology*, *38*, 1206–1222.

Tegen, I., Lacis, A. A., & Fung, I. (1996). The influence on climate forcing of mineral aerosols from disturbed soils. *Nature*, *380*, 419–422.

Thallaid, V. R., Nüsse, M., & Boese, R. (2000). The melting point alteration in α,ω-alkanedicarboxylic acids. *Journal of American Chemistry Sociality*, *122*, 9227–9236.

Topping, D.O., McFiggans, G. B., Kiss, G., Varga, Z., Facchini, M. C., Decesari, S., & Mircea, M. (2006). Surface tensions of multi-component mixed inorganic/organic aqueous systems of atmospheric significance: Measurements, model predictions and importance for cloud activation predictions. *Atmospheric Chemistry and Physics Discussions*, *6*, 12057–12120.

Weingartner, E., Burtscher, H., & Baltensperger, U. (1997). Hygroscopic properties of

carbon and diesel soot particles. *Atmospheric Environment*, *31*, 2311–2327.

Xue, H., Khalizov, A. F., & Zhang, R. (2008a). Effect of dicarboxylic acid coating on the mass-mobility relationship of soot particles. *Environmental Science and Technology*, submitted.

Xue, H., Khalizov, A. F., & Zhang, R. (2008b). Organic coatings and their enhancement of optical properties on soot aerosols. in preparation.

Zhang, D., & Zhang, R. (2005). Laboratory investigation of heterogeneous interaction of sulfuric acid with soot. *Environmental Science and Technology*, *39*, 5722–5728.

Zhang, R., Khalizov, A. F., Pagels, J., Zhang, D., Xue, H., & McMurry, P. H. (2008) Variability in morphorlogy, hygroscopicity, and optical properties of soot aerosols during atmospheric processing. *Proceedings of the National Academy of Sciences USA*, *105*, 10291–10296.

Zuberi, B., Johnson, K. S., Aleks, G. K., Molina, L. T., & Molina, M. J. (2005). Hydrophilic properties of aged soot. *Geophysical Research Letters*, *32*, L01807, doi:10.1029/2004GL021496.

VITA

Name: Huaxin Xue

Address: Department of Atmospheric Sciences, Texas A&M University

College Station, TX 77843-3150, United States

Email Address: huaxin.xue@yahoo.com

Education: M.S., Atmospheric Sciences, Texas A&M University, 2009

M.S., Environmental Science, Fudan University, 2003

B.E., Environmental Engineering, Donghua University, 1998